Numerical modeling of the late Cenozoic geomorphic evolution of Grand Canyon, Arizona

Jon D. Pelletier†
Department of Geosciences, University of Arizona, Gould-Simpson Building, 1040 East Fourth Street, Tucson, Arizona 85721-0077, USA

ABSTRACT

The late Cenozoic geomorphic evolution of Grand Canyon has been influenced by three primary tectonic and drainage adjustment events. First, 1 km of relief was produced along the Grand Wash–Wheeler Fault system beginning at 16.5 Ma. Second, the ancestral Colorado River became integrated with the lower Colorado River through Grand Canyon between 5.5 and 6 Ma. Third, the Colorado River was influenced by Plio-Quaternary normal faulting along the Hurricane and Toroweap Faults. Despite the relatively firm constraints available on the timing of these events, the geomorphic evolution of Grand Canyon is still not well constrained. For example, was there a deeply incised gorge in western Grand Canyon before Colorado River integration? How did incision rates vary through time and along the evolving river profile? What is the role of isostatic rebound and Plio-Quaternary faulting on the recent incision history of Grand Canyon? In this paper I describe the results of a process-based numerical modeling study designed to address these questions and to determine the plausibility of different proposed models for the erosional history of Grand Canyon. The numerical model I developed integrates the stream-power model for bedrock channel erosion with cliff retreat and the flexural-isostatic response to erosion. Two end-member paleodrainage and integration scenarios are considered. In the first model, I assume no incision in western Grand Canyon prior to 6 Ma. This model is equivalent to a lake-overtopping scenario for Colorado River integration. In this scenario, the model predicts that Colorado River integration at 6 Ma initiated the formation of a large (700 m) knickpoint that migrated headward at a rate of 100 km/Ma, resulting in rapid incision of western Grand Canyon down to the level of the Redwall Limestone from 6 to 4 Ma and incision of eastern Grand and Marble Canyons from 4 to 2 Ma. Widening of Grand Canyon by cliff retreat triggered flexural-isostatic rebound and renewed river incision of up to 350 m in Plio-Quaternary time according to this model. The model also indicates that Plio-Quaternary normal faulting significantly dampened incision rates in western Grand Canyon relative to eastern Grand Canyon. In the second paleodrainage scenario, I assume that a 13,000 km^2 paleodrainage crossed the Grand Wash–Wheeler Fault system at 16.5 Ma. The results of this model scenario indicate that relief production along the Grand Wash–Wheeler Fault system could have initiated the formation of a large (700 m) knickpoint that migrated headward at a rate of 15 km/Ma prior to 6 Ma to form a 150-km-long gorge in western Grand Canyon. Following integration at 6 Ma, the results of this model scenario are broadly similar to those of the first model, i.e., rapid incision through Grand and Marble Canyons from 6 to 2 Ma followed by cliff retreat, isostatic rebound, and fault-controlled incision. The results of the second model scenario illustrate that headward erosion of a proto–Grand Canyon could have been sufficient to capture the ancestral Colorado River east of the Shivwitz Plateau.

INTRODUCTION

The past decade has seen renewed interest in the late Cenozoic geomorphic history of Grand Canyon. The availability of new geochronometers has primarily fueled this interest. Alluvial terraces (Pederson et al., 2002, 2006), travertine deposits (Abbott and Lundstrom, 2007), and basalt flows (Pederson et al., 2002; Karlstrom et al., 2007) have provided firm constraints on the Plio-Quaternary history of river incision. Plio-Quaternary incision rates measured by these studies are lower than late Cenozoic rates (determined by dividing the total depth of incision into the Kaibab Limestone by 6 Ma) (Pederson et al., 2002) and incision rates from 0.5 to 4 Ma are two to three times higher in eastern Grand Canyon compared to western Grand Canyon (Karlstrom et al., 2008). Pederson et al. (2002) and Karlstrom and Kirby (2004) argued that lower incision rates measured in western Grand Canyon were the result of the relative subsidence of the western Grand Canyon block due to offset along the Hurricane and Toroweap Faults. Higher incision rates in eastern Grand Canyon could also be a consequence of knickpoint propagation, however. The relationship between Plio-Quaternary incision rates and the longer-term history of river incision is still unclear, in part due to the complexity of the geomorphic processes involved, including bedrock channel erosion, cliff retreat, the flexural-isostatic response to erosional unloading, and the interaction of each of these processes with Plio-Quaternary normal faulting. Numerical modeling, calibrated with geochronology, can be a powerful tool for quantifying these complex geomorphic processes and for using the detailed knowledge of recent incision rates to better understand the longer-term geomorphic evolution of bedrock-dominated river systems (e.g., Pelletier, 2007).

The erosional history of the Grand Canyon region has been influenced by three major tectonic and drainage adjustment events since 16.5 Ma (Fig. 1). First, extension along the Grand Wash–Wheeler Fault system from 16.5 to 13 Ma resulted in relief production between the Colorado Plateau and the Grand Wash Trough (Faulds et al., 1990). The topographic step created along this fault system triggered incision of drainages flowing across it (Faulds et al., 2001). The depth and width of that incisional response to offset is not well constrained, but speleothem records of groundwater-table elevations in western Grand Canyon suggest that a proto–Grand Canyon began carving down to the level of the Redwall Limestone at 16 Ma (Hill et al., 2001; Polyak et al., 2008). The speleothem records are controversial, however, because

†E-mail: jdpellet@email.arizona.edu

GSA Bulletin; March/April 2010; v. 122; no. 3/4; p. 595–608; doi: 10.1130/B26403.1; 13 figures.

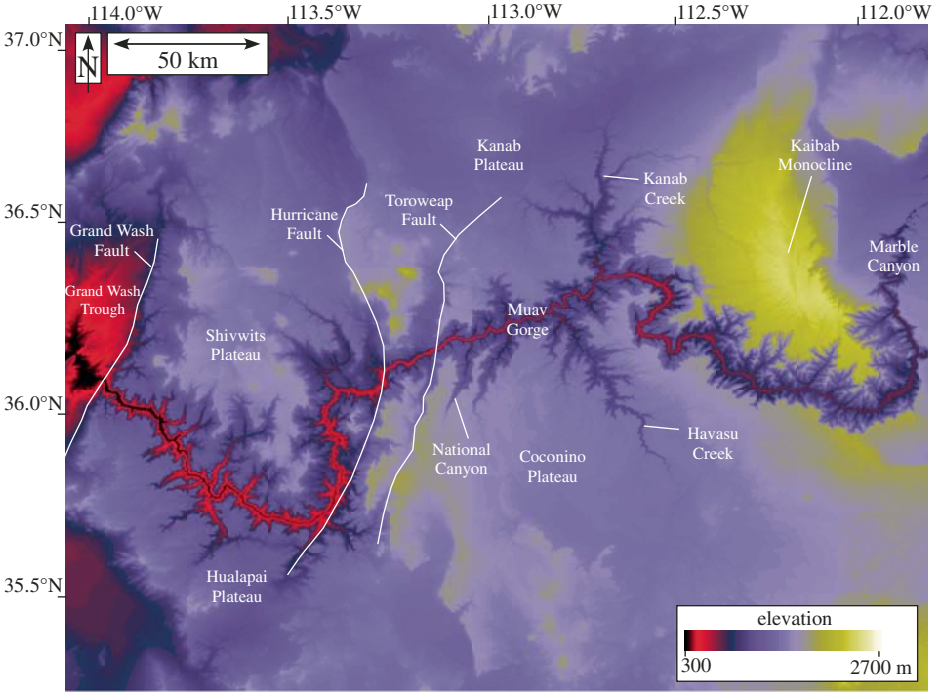

Figure 1. Color map of the topography of the Grand Canyon region, showing the location of major geomorphic and structural features.

groundwater tables in western Grand Canyon could have lowered due to offset along the Grand Wash–Wheeler Fault system rather than by incision in western Grand Canyon (Pearthree et al., 2008; Pederson et al., 2008). Sediments of the Muddy Creek Formation indicate that the upper Colorado River was not integrated with the Grand Wash Trough until 5.5–6 Ma (Spencer et al., 1998; Faulds et al., 2001). Following integration, it is not known whether incision by the Colorado River took place predominantly by upstream migration of a steep knickpoint or by spatially uniform downcutting, but evidence for high rates of Quaternary incision in Marble and Glen Canyons (Davis et al., 2001; Hanks et al., 2001; Cook et al., 2009) suggest that the Colorado River may have incised as a steep, eastward-propagating knickpoint from 6 Ma to the present. Upstream from Glen Canyon, channels draining the San Juan Mountains do not appear to have been influenced by Grand Canyon incision (Wolkowinsky and Granger, 2004), suggesting that Lees Ferry represents the farthest upstream location of the knickpoint that excavated Grand Canyon (Karlstrom and Kirby, 2004). The Hurricane and Toroweap Faults have produced a total of nearly 600 m of normal fault offset in the Plio-Quaternary period (Wenrich et al., 1997). Pederson et al. (2002) associated this fault activity with lower rates of Quaternary incision in western Grand Canyon relative to eastern Grand Canyon. Hanks and Blair (2002), however, argued that the effect of offset along these faults would be limited to a fairly short distance (i.e., <30 km) downstream from each fault.

Little is firmly known about how the ancestral Colorado River became integrated with the Grand Wash Trough at 6 Ma. The prevailing view is that the ancestral Colorado River terminated in a lake on the Colorado Plateau and that spillover of this lake at 6 Ma initiated the incision of western Grand Canyon (Blackwelder, 1934; Meek and Douglass, 2001; Scarborough, 2001; Spencer and Pearthree, 2001; Pederson, 2008). Where and how this lake formed and drained is not well constrained, however. Spencer and Pearthree (2001) argued that headward erosion of a proto–Grand Canyon could not have occurred fast enough to have captured the ancestral Colorado River east of the Shivwitz Plateau. As such, they propose that water from the ancestral Colorado River most likely ponded into a lake that grew deep enough to drain catastrophically over the southeastern limb of the Kaibab Monocline to begin carving the Grand Canyon at 6 Ma. Basin morphological analysis, however, suggests that the best candidate for the deposits of such a lake east of the Kaibab Monocline, i.e., the Bidahochi Formation, did not have sufficient accommodation space to have been the primary depozone for a river of that size (Dallegge et al., 2001). Recently, Pederson (2008) argued that the Muddy Creek Formation in the Lake Mead area was the likely site of mid-late Miocene deposition of the ancestral Colorado River prior to integration with the Grand Wash Trough. If so, lake spillover or groundwater-driven piracy east of the Shivwitz Plateau and west of the Kaibab Monocline could have caused integration (Pederson, 2008; Hill et al., 2008). Recent thermochonologic results indicate that a 1-km-deep incised canyon existed in the post-Paleozoic sedimentary rocks atop the Kaibab Monocline (Flowers et al., 2008; Lee, 2007). These results are relevant to the question of how the Colorado River became integrated because they suggest that the Colorado River could have been superposed on the Kaibab Monocline. Headward erosion of a proto–Grand Canyon is favored by some, in part, because it helps to explain the "problem" of how the Colorado River "crossed" the Kaibab Monocline at its highest structural point. The results of Flowers et al. (2008) and Lee (2007), however, suggest that this "Kaibab-crossing" problem may not, in fact, be a problem (Pederson, 2008).

An alternative view is that the ancestral Colorado River was captured by a headward-eroding "proto–Grand Canyon." McKee et al. (1967) proposed that this capture event took place near the Kaibab Monocline. Spencer and Pearthree (2001) argued against this mechanism based on characteristic rates of scarp retreat in arid climates. Headward erosion of a proto–Grand Canyon would have been driven by drainage basin runoff, however, and hence scarp retreat by mass wasting is not an appropriate comparison. The headward-erosion scenario for integration suffers from limited constraints on the size of the paleodrainage system that drove headward erosion. Young (2008) argued that this paleodrainage was >13,000 km^2 in area based on his assessment of the Miocene paleogeography, but this value is not well constrained. If a deeply incised canyon of significant size did exist in western Grand Canyon prior to 6 Ma, it is reasonable to expect that such a canyon would have deposited large volumes of clastic debris in the Grand Wash Trough and its adjacent basins. The sediments in this area are well exposed and well studied and clearly contain only a very limited volume of clastic material (Longwell, 1946). This volume constraint is known as the "Muddy Creek problem."

Young (2008) recently argued that the limited volume of clastic debris in the Muddy Creek Formation is not as firm a constraint on the size of the proto–Grand Canyon as previous studies have concluded, however. The volume of clastic debris in the Muddy Creek Formation provides no direct constraint on the length of a

proto–Grand Canyon, only its volume. It is the length of such a canyon that is most important for determining whether headward growth could have led to capture of the ancestral Colorado River. Young (2008) pointed out that some of the clastic debris excavated from a proto–Grand Canyon could have been stored temporarily upstream from the mouth of the proto–Grand Canyon between 11 and 6 Ma, thus relieving some, but not all, of the volume problem. Some of the clastic debris excavated from a proto–Grand Canyon could have been transported out of the Grand Wash Trough by eolian processes during periods of low lake level and, later, to the ocean by fluvial processes. The majority of the basin-floor deposits of the lower Colorado River and its adjacent areas are Quaternary in age. The limited preservation of once-extensive Pliocene deposits in these areas is a testament to how much fluvial reworking has taken place between Pliocene and Quaternary time (Howard et al., 2008). Finally, as noted by Young (2008), a significant portion of the rock excavated from western Grand Canyon is Paleozoic limestone. As such, some of this rock dissolves and does not produce clastic debris. Given late Holocene dissolution rates of carbonate boulders in Grand Canyon (Hereford et al., 1998), ca. 200 ka is required to completely dissolve a limestone boulder 1 m in diameter under present climatic conditions. $^{87}Sr/^{86}Sr$ ratios, however, suggest that springs were the dominant source for the Hualapai Limestone (Crossey et al., 2009). While it is generally accepted that the volume of clastic sediment in the Muddy Creek Formation rules out a proto–Grand Canyon of any significant size, these considerations suggest that further consideration of the headward-erosion mechanism for integration is warranted.

In this paper I use numerical modeling to address the following questions: was there a deeply incised gorge in western Grand Canyon before Colorado River integration? If so, is this proto–Grand Canyon necessary to explain the geometry and incision history of the modern Grand Canyon? Using stream-power erosion laws, how did incision rates vary through time (steady or time-varying), and how did incision rates vary along the evolving stream profile? What is the role of isostatic rebound and Plio-Quaternary faulting on the recent incision history of Grand Canyon? In the model I consider two end-member paleodrainage scenarios: one that assumes no incision in western Grand Canyon prior to 6 Ma and another that assumes a 13,000 km^2 paleodrainage as proposed by Young (2008). In the first model, lake overtopping is not modeled explicitly, but instead the model abruptly introduces the full discharge of the Colorado River at 6 Ma, triggering upstream propagation of a knickpoint starting at the Grand Wash–Wheeler Fault system. As such, this model scenario is representative of a lake-overtopping scenario in terms of how such an instantaneous introduction of discharge would initiate incision into the "rim surface" of Grand Canyon. In the second model scenario, knickpoint propagation begins at 16 Ma with offset along the Grand Wash–Wheeler Fault system but proceeds more slowly compared to the first model due to its much smaller 13,000 km^2 paleodrainage. This second model scenario provides a specific evaluation of the Young (2008) and Spencer and Pearthree (2001) conclusions that such a proto–Grand Canyon could (Young, 2008) or could not (Spencer and Pearthree, 2001) have grown headward to capture the ancestral Colorado River at a point east of the Shivwitz Plateau by 6 Ma.

MODEL DESCRIPTION

Modeling the erosional response to base-level drop requires mathematical models for hillslope and bedrock channel erosion. The classic method for quantifying bedrock channel erosion, the stream-power model, assumes that bedrock channel erosion is proportional to excess stream power, i.e., the product of unit discharge and channel-bed slope minus a threshold value:

$$\begin{aligned} \frac{\partial h}{\partial t} &= U - K\frac{Q}{w}\left|\frac{\partial h}{\partial x}\right| + K'\tau \quad \text{if} \quad K\frac{Q}{w}\left|\frac{\partial h}{\partial x}\right| > K'\tau \\ \frac{\partial h}{\partial t} &= U \qquad\qquad\qquad\qquad\quad \text{if} \quad K\frac{Q}{w}\left|\frac{\partial h}{\partial x}\right| \le K'\tau \end{aligned}, \quad (1)$$

where h is local elevation, t is time, U is uplift rate, K is the coefficient of bedrock erodibility, Q is discharge, w is channel width, x is the along-channel distance, and $K'\tau$ is a threshold value that must be exceeded for erosion to take place (Whipple and Tucker, 1999). Scaling relationships between discharge, channel width, and drainage area can be used to further simplify equation 1 to:

$$\begin{aligned} \frac{\partial h}{\partial t} &= U - KA^m\left|\frac{\partial h}{\partial x}\right| + K'\tau \quad \text{if} \quad KA^m\left|\frac{\partial h}{\partial x}\right| > K'\tau \\ \frac{\partial h}{\partial t} &= U \qquad\qquad\qquad\quad \text{if} \quad KA^m\left|\frac{\partial h}{\partial x}\right| \le K'\tau \end{aligned}, \quad (2)$$

where A is drainage area and m is an exponent that combines the scaling relationships between discharge, channel width, and drainage area (note that the coefficient K in equations 1 and 2 have different values and different units after equation 1 is transformed into equation 2). The stream power model is most applicable to the erosion of sedimentary rocks. Field evidence suggests that the dominant erosional process in jointed sedimentary rock is the plucking of rock from the channel bed during extreme floods (Whipple et al., 2000). Recent work, however, has also emphasized the importance of the saltation abrasion process in bedrock channel erosion (Sklar and Dietrich, 2004). In massive lithologies such as granite, plucking is not effective and channel incision is likely to be dominated by abrasion. Given that the majority of the Grand Canyon sequence is comprised of Paleozoic sedimentary rocks, however, the stream power model is the more appropriate model for quantifying bedrock incision in this case. Calibration of each of the terms in equation 2 for the Grand Canyon region is described in detail in the Model Calibration section.

Hillslopes adjacent to the bedrock channels of Grand Canyon are dominated by cliff and talus slopes. Arid-region cliffs evolve predominantly by slope retreat, i.e., cliffs retreat laterally through time while maintaining their shape. This type of evolution is in marked contrast to the predominantly diffusive evolution common in humid and/or low relief landscapes. The cliff-retreat process can be modeled using an advection equation (Lange, 1959; Luke, 1972):

$$\frac{\partial h}{\partial t} = U - C|\nabla h|, \quad (3)$$

where C is the rate of cliff retreat. Equation 3 is also known as the "one-way" wave equation because it has a form similar to that of the classical wave equation, except that topographic waves propagate in one direction (upslope) only. Equation 3 has been used to model cliff retreat in Grand Canyon in three of the earliest examples of numerical landform evolution models (Lange, 1959; Pollack, 1969; Aronsson and Linde, 1982). It should be noted that equation 3 does not explicitly include the storage of colluvium on talus slopes. As such, the model of this paper assumes that colluvial storage is negligible over the geologic time scales of canyon formation. The transition between hillslopes and channels in the model occurs when the drainage area is greater than a threshold value A_c, calibrated in the section below. Equations 2 and 3 can be solved using the upwind differencing method coupled with an adaptive time step that ensures computational efficiency and numerical stability (Press et al., 1992; Pelletier, 2008).

Any numerical model of landform evolution in Grand Canyon must honor the structural geology of the region at least to first order. The structural geology of the southwestern Colorado Plateau includes rock types with varying resistance to erosion as well as significant Plio-Quaternary offset along the Hurricane and

Toroweap Faults (Fig. 2). The variable rock types of the Paleozoic stratigraphy and the older Precambrian units of Grand Canyon require that the bedrock erodibility coefficients, K, vary spatially. Because the deformed stratigraphy closely parallels the modern topographic surface, K can be approximated as a function of the depth of incision into the modern "rim surface," denoted by h_{rs}, which corresponds closely with the structural surface of the Kaibab Limestone. In principal, each layer of the Paleozoic stratigraphy and older Precambrian rocks is characterized by its own values of K. In practice, however, three major structural groups exert the predominant control on spatial variations in K: the resistant units of Kaibab Limestone through Coconino Sandstone, the weaker units of the Hermit Shale through Supai Group, and the resistant units of the Redwall Limestone and underlying rocks. Evidence for similar bedrock erodibility coefficients within each of these groups is presented in the Model Calibration section below.

Fault offset in the model is assumed to occur in two periods. First, 700 m of vertical offset is produced along the Grand Wash Fault from 16 to 13 Ma. This magnitude of offset assumes that 700 out of the total 1300 m of modern topographic relief between the Colorado Plateau and the Grand Wash Trough were produced by late Miocene offset along the Grand Wash Fault. Structural offset along the Hurricane (400 m) and Toroweap Faults (nearly 200 m) (Jackson, 1990; Wenrich et al., 1997; Billingsley and Wellmeyer, 2003) constrain the remaining 600 m produced by Plio-Quaternary offset along the Hurricane and Toroweap Faults. In the model I assume that both the Hurricane and Toroweap Faults develop their respective offsets with uniform rates between 4 Ma and the present. The 4 Ma initiation age of faulting is not directly constrained, but late Quaternary slip rates of ~100 m/Ma (Fenton et al., 2001) along the Hurricane Fault imply an initiation age of ca. 4 Ma, if the slip rate along this fault (the larger of the two) has been constant since initiation. In the model, fault offset rates are assumed to decrease over a distance of 120 km north and south of where the Colorado River crosses the fault zone. By including this assumption, the fault offsets approach zero along the northern and southern edges of the model domain.

The model also includes the flexural-isostatic response to erosion by solving for the deflection of a thin elastic plate with uniform elastic thickness subject to vertical unloading:

$$D\nabla^4 w + \Delta\rho g w = q(x, y), \tag{4}$$

where w is the deflection (rock uplift), D is the flexural rigidity, $\Delta\rho$ is the density contrast between the crust and the mantle, g is the acceleration due to gravity, and $q(x,y)$ is the weight of the rock removed by erosion (Watts, 2001). Equation 4 can be used to solve for the rock uplift in response to the erosional removal of part of the topographic load. The average elastic thickness of the Colorado Plateau is 22 km and ranges from 12 to 37 km (Lowry and Smith, 1995). The elastic thickness of western Grand Canyon specifically (the area of the model where most of the erosional unloading takes place in the model) is ~10–20 km based upon the map presented in Lowry et al. (2000). In the model I assume a uniform value of 10 km for T_e. I chose a value at the low end of this range based on the fact that Plio-Quaternary normal faulting will reduce the effective strength of the lithosphere in the late stages of the model when erosional unloading is most rapid. This value was then converted to a flexural rigidity, D, using the relationship

$$D = \frac{ET_e^3}{12\left(1-\nu^2\right)}, \tag{5}$$

where E = 70 GPa and ν = 0.25 (typical values for continental lithosphere), before input to the model. Equation 4 was solved in the model using the Fourier transform technique (Press et al., 1992; Pelletier, 2008).

The initial condition of the model at 16 Ma assumes that the middle-late Miocene topography of the region coincides with the modern rim surface formed on the Kaibab Limestone, minus the offset along the faults and flexural-isostatic uplift. This initial topography, $h_{t=0}$, was created from the modern topography, h_{obs}, using the function:

$$h_{t=0} = \begin{cases} h_{obs} - 150 & \text{if } h_{obs} > 1700 \\ (1700 - h_{obs})/10 - 150 & \text{if } h_{obs} < 1700 \end{cases}. \tag{6}$$

The "modern topography" is given by the 30 m/pixel U.S. Geological Survey digital elevation model (DEM) of the region, subsampled

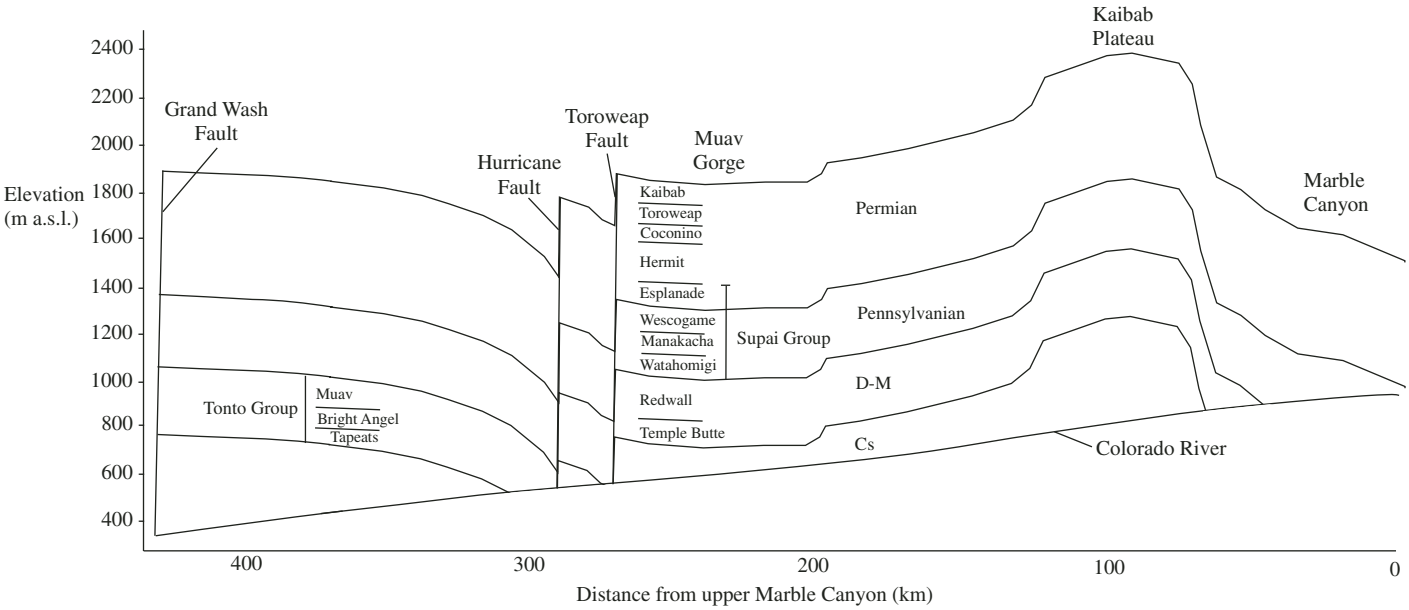

Figure 2. Structural cross section of the modern Grand Canyon from Marble Canyon (far right) to the Grand Wash Trough (far left), after Pederson et al. (2003). The numerical model honors the fault architecture and Paleozoic rock types illustrated in the cross section.

to the pixel resolution of the model (i.e., 90 m). Equation 6 effectively "fills" the incised canyons to near the 1700 m contour (i.e., approximately the lowest elevations of the plateaus surrounding Grand Canyon) and lowers the relief of the Hurricane and Toroweap Cliffs, but retains the high-elevation topography of the Kaibab Monocline because this feature was formed in the Laramide and hence was present in the mid-late Miocene landscape. Equation 6 also lowers the initial plateau topography by 150 m, which is a spatially averaged value for the late Cenozoic flexural-isostatic rebound produced by the model.

Two alternative scenarios are used for drainage architecture in the model, reflecting the uncertainty that exists in the Miocene paleogeography of the region and the controversy over whether or not an incised canyon of significant size could have existed in western Grand Canyon in middle-late Miocene time. In both models, the upper Colorado River is "removed" from the model prior to 6 Ma by placing a divide along the present course of the Colorado River on the southeast side of the Kaibab Monocline. After 6 Ma, the divide separating the upper Colorado River from the rest of the model domain is removed, "introducing" the river back into the system where it flows down the topographic gradients set by the course of the modern Colorado River via equation 6 (Fig. 3). Flow routing in the model is performed using the multiple-flow direction algorithm of Freeman (1991). It is important to emphasize that removing the upper Colorado River by placing a paleodivide in the model is simply a convenient way to "introduce" the Colorado River into the model at 6 Ma along the path that it must have taken to carve the modern Grand Canyon. The location of the paleodivide placed into the model on the southeastern side of the Kaibab Monocline prior to 6 Ma is not necessarily where or when the Colorado River crossed the Kaibab Monocline, however. The Colorado River could have crossed the Kaibab Monocline earlier than 6 Ma, but without the relief associated with flow over the Grand Wash Cliffs, the river would not have incised into the Kaibab surface along whichever course it took. Precisely how and when the Colorado River crosses the Kaibab Monocline does not affect the behavior of the model of this paper because canyon cutting by the Colorado River only occurs once integration with the Grand Wash Trough takes place at 6 Ma. In the first model scenario (herein called model 1), no erosion is assumed to take place prior to 6 Ma. In the second model scenario (model 2), a drainage area of 13,000 km^2 is assumed in western Grand Canyon prior to 6 Ma based on the paleogeographic reconstruction of Young (2008). In mid-Miocene time, the topographic and structural dips of the Kaibab surface were oriented northeast. As a result, runoff routed through the Grand Wash Cliffs would have been sourced primarily from the Hualapai and Coconino Plateaus. Young (2008) estimated the contributing area of this likely Miocene drainage to be 13,000 km^2. In the model, I first calculate the contributing area through each pixel in the model domain using the modern topography with the upper Colorado River "removed" using the paleodivide placed into the model. This initial flow routing step yields a drainage area of ~22,000 km^2. The drainage area values in the model are then scaled by the ratio of 13,000 to 22,000 km^2 at every point, thereby resulting in a drainage configuration in western Grand Canyon that matches the Miocene paleotopography (i.e., northeast-dipping Hualapai and Shivwitz Plateaus, similar to today) and creates a proto–Grand Canyon with the same drainage area estimated by Young (2008). An alternative approach would have been to place multiple divides along the north rim of Grand Canyon to "shut off" the flow that contributes to the discharge in the canyon today but most likely did not contribute to the Miocene proto–Grand Canyon.

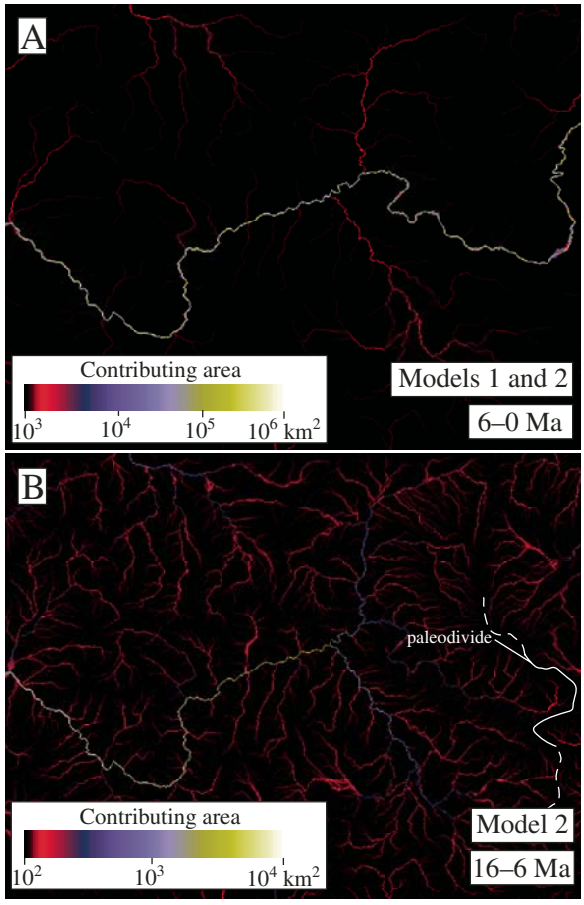

Figure 3. Color maps of drainage area (A) after and (B) before integration of the Colorado River at 6 Ma (note logarithmic color scale). In (B), a paleodivide was placed into the U.S. Geological Survey digital elevation model (DEM) of Grand Canyon along the southeast limb of the Kaibab Monocline in order to separate the upper and lower Colorado drainage basins for the purposes of the model. Note that in (B) the drainage area is several orders of magnitude lower than in (A) (reflecting the lack of drainage from east of the Kaibab Monocline prior to 6 Ma), and the drainage area decreases to zero at the paleodivide.

MODEL CALIBRATION

In order to calibrate the value of A_c, the threshold area for channelization, it is necessary to identify some diagnostic measure of the topography that is different between hillslopes and channels, and then calculate that measure as a function of area to identify a threshold value that characterizes the hillslope-channel transition in this study area. A classic method of constraining the threshold drainage area for channelization is the slope-area relationship (Tucker and Bras, 1998). The average channel slope for a given drainage area is often found to be an inverse power-law function of area. Near the hillslope-channel threshold, however, there is often a "rollover" in the slope-area plot that represents the transition from channels to hillslopes. This rollover reflects the transition from concave channels to convex (or planar) hillslopes. This approach does not work in Grand Canyon because there is no rollover in the slope-area plot, even down to drainage areas equal to a single pixel. The reason for this continuous scaling of slope versus area down to the smallest scales is most likely that it is the result of the extreme hillslope relief in Grand Canyon. As

an alternative to the slope-area approach, I computed the local curvature, or Laplacian, of the topography, $\nabla^2 h$, in all pixels of the 30 m/pixel DEM of Grand Canyon (surrounding plateaus excluded) and plotted that data as a function of drainage area (Fig. 4). The idea behind this approach is that hillslopes in Grand Canyon can be expected to have lower curvature values relative to channels because hillslopes are generally more planar, thus yielding low curvature values, compared to the V-shaped, cross-sectional profiles characteristic of fluvial channels, which yield significantly higher curvature values. The plot of curvature (averaged for all pixels with the same drainage area) as a function of drainage area shows a "kink" in the plot at $A_c = 0.3$ km^2. Therefore, I used 0.3 km^2 as the value for A_c in the model. Sensitivity studies of the model, however, indicate that the model results are very insensitive to the specific value of A_c over a wide range of reasonable values, i.e., from 0.05 to 2 km^2. This insensitivity reflects the fact that, at sufficiently small scales, cliff retreat dominates over bedrock channel erosion in the model.

In order to calibrate the value of m, data for the relationships between peak discharge and drainage area and channel width and drainage area are needed. The relationship between peak discharge and drainage area, in particular, depends on climate and must be constrained on a site-specific basis. Baker (2006) compiled data for peak discharge and drainage area in the Colorado Plateau region of Arizona and found that peak discharges scale with drainage area to the 0.73 power. The sublinear relationship between peak discharge and drainage area in this region reflects hydrological loss mechanisms that are more effective per unit area in larger drainage basins (i.e., infiltration and evapotranspiration) compared to small drainage basins, as well as the fact that storms of larger area generally have a lower average precipitation intensity. Peak discharge was used in this analysis because most of the geomorphic work of bedrock channel erosion in arid environments occurs during large, rare flood events. It is the largest discharges observed over time scales of centuries to millennia, not the typical or mean annual discharges, that best represent the geomorphically most effective flood events. Compilations of available data sets for the relationship between channel width and drainage area yield a scaling relationship with a best-fit exponent of 0.36 (Whipple, 2004). This relationship has been confirmed by later studies (e.g., Wohl and David, 2008). Combining the 0.73 and 0.36 exponents between discharge and drainage area and channel width and drainage area, respectively, provides a calibration value of $m = 0.50$ for active bedrock incision on the Colorado Plateau region in Arizona. It is now well established that relationships between channel width and discharge depend on incision rate (Finnegan et al., 2005; Whittaker et al., 2007); hence the uniform scaling relationship between channel width and drainage area assumed in the model is not correct in detail. However, incision rates in the model are generally low except during time periods when knickpoints are actively retreating past a given point. Since most of the excavation of Grand Canyon occurs during this "incising" phase, a single scaling law that accurately represents that phase will accurately represent the majority of Grand Canyon's downcutting history.

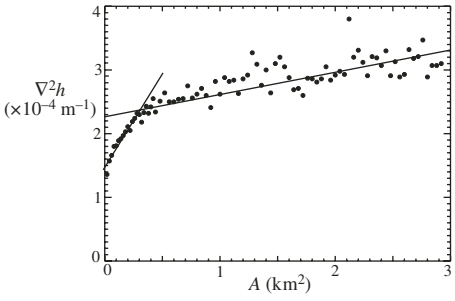

Figure 4. Plot of average curvature versus drainage area computed using a 30 m/pixel U.S. Geological Survey digital elevation model (DEM) of Grand Canyon. The plateaus surrounding the Grand Canyon were excluded from the analysis. The data show a kink in the curve at $A_c = 0.3$ km^2, representing the transition from planar hillslopes to concave channels.

The relative erodibility of the Paleozoic and Precambrian rocks of Grand Canyon can be estimated using the longitudinal profiles of the major side canyons to the Colorado River. In topographic steady-state (i.e., $\partial h/\partial t = 0$), equation 2 can be rearranged to infer the relative erodibility by normalizing the slope by a function of drainage area:

$$K = \frac{U + K'\tau}{SA^m}, \qquad (7)$$

where S is the along-channel slope. The side canyons of the Colorado River in Grand Canyon are *not* in topographic steady state, but equation 7 can still be used to estimate the relative erodibility coefficients of different structural zones using an iterative approach. In this approach, equation 7 provides a preliminary estimate of the relative values of K corresponding to each distinct erodibility zone. Then, the results of the model are used as a consistency check on the preliminary estimates. According to equation 7, values of K should be approximately inversely proportional to the product of channel slope and the square root of drainage area. In the side tributaries of Grand Canyon, plots of $SA^{0.5}$ along the channel profile illustrate three distinct erodibility zones (Fig. 5). In Havasu and National Canyons, the top 300 m of the canyon stratigraphy is dominated by relatively resistant units (i.e., a relatively high $SA^{0.5}$ value). The next 400 m in the stratigraphy are dominated by units approximately five times weaker (i.e., a $SA^{0.5}$ value five times lower). The lowest segment of the canyon stratigraphy (i.e., depths of greater than 700 m) has approximately the same erodibility as the top 300 m. Using this approach, I estimated relative erodibility coefficients of 1:5:1 for incision depths less than 300 m, between 300 and 700 m, and greater than 700 m, respectively (Fig. 5). In some locations, exposure of basement rocks and the Bright Angel Shale can be expected to modify the erosional resistance of the lowermost levels of the structural profile, and more complex structural models that incorporate these and additional units could be developed. Model-predicted profiles for these canyons are quite similar to the actual profiles (Fig. 5), thus providing a post–model-development validation or self-consistency check on these initial estimates. Using the observed side canyon profiles as calibration data for the model has an important advantage that should be noted. Channel widths in bedrock river systems scale with drainage area, but they are also strongly controlled by rock strength in areas where rock strength varies spatially. By using the observed channel profiles within a stream-power context, rock-strength controls on channel width are implicitly included in the calibration procedure. If channels carving through the strong units of the Grand Canyon sequence are uniformly narrower for a given contributing area compared to channels in weaker rocks, that effect will be included in the lower relative values of K obtained for those rocks using this calibration procedure.

In order to constrain the absolute values of K, the relative values for each of the three erodibility units were scaled up and down in order to match the observed extent of headcutting along the two major side canyons to Grand Canyon (i.e., Kanab and Havasu Creeks). If the absolute value of K is set too high in the model, the extent of headcutting in these two canyons predicted by the model will be unrealistically large, given the model duration of 6 Ma (model 1) or 16 Ma (model 2). If the absolute value of K is set too small, the side canyons do not extend as far upstream as we observe them today. By modifying the absolute value of K in an iterative manner, the appropriate scaling factor for K was determined by requiring consistency between the model and the observed position of maximum

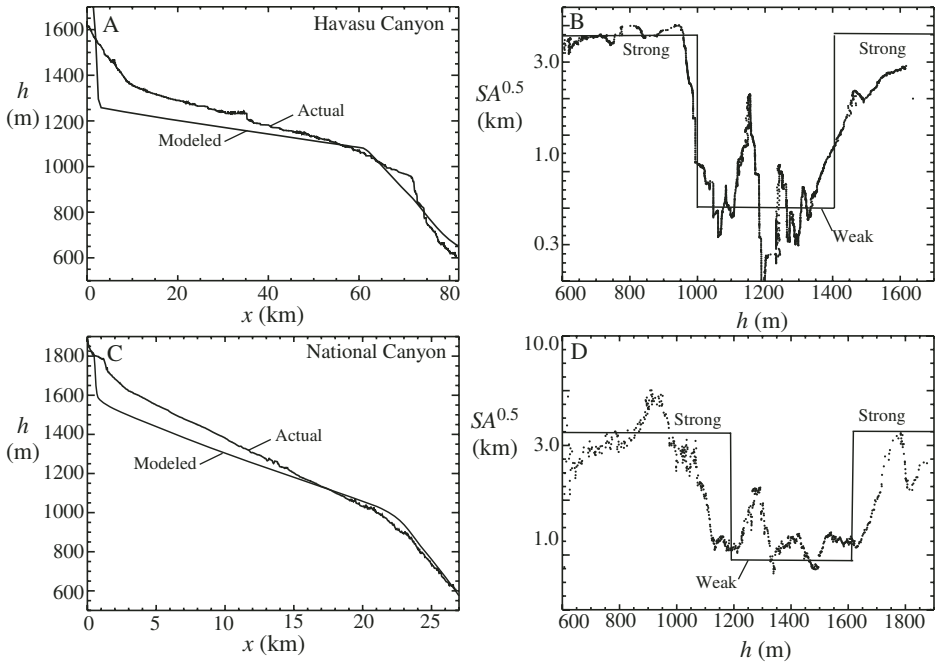

Figure 5. Slope-area scaling of side tributaries to the Colorado River in Grand Canyon. (A–B) Havasu Canyon; (C–D) National Canyon. (A) Longitudinal profile of Havasu Canyon, illustrating the three-tiered stratigraphy of strong (Kaibab through Coconino), weak (Hermit through Supai Group), and strong (Redwall and lower) erodibility zones of Grand Canyon. (B) Plot of $SA^{0.5}$ as a function of elevation h, with the model simplification of three zones (strong:weak:strong) as a function of distance below the rim. (C–D) Same as (A–B) but for National Canyon. Note that in (A) and (C) the modeled profiles are superimposed on the actual profiles, providing a post–model-development validation of this approach.

headcutting along Kanab and Havasu Creeks. Using this iterative procedure, optimum values of $K = 1.5 \times 10^{-4}$ and 7.5×10^{-4} ka^{-1} were determined for the strong and weak units of the canyon, respectively, for model 1. For model 2, the constrained values of K decrease to 1.2×10^{-4} and 6.0×10^{-4} ka^{-1}, respectively. Higher values of K are required for model 1 because this model has less time to propagate the Kanab and Havasu headcuts to their present locations compared to model 2. It should be emphasized that the goal of this model is to constrain the *past* evolution of the Grand Canyon system. In this context, it is appropriate to use aspects of the modern topography as observational constraints that the model must honor. In other words, it may seem circular to use the modern topography of Grand Canyon as a calibration constraint on the model, but as long as the purpose of the model is to constrain the past evolution of Grand Canyon, the modern topography is just as valid a constraint as recent incision rates or any other measurement of the state of the system at a known point in time.

The approach of calibrating the absolute values of K using the modern extent of side-canyon headcutting has another important advantage that should be emphasized. At certain times in the geologic past and in certain segments of the river, alluvium has been episodically stored on the channel bed. In using a bedrock erosion model in this paper, I am not suggesting that the Colorado River and its tributaries have never stored alluvium on the channel bed. Rather, I am assuming that the alluvial storage that has taken place along the river for certain periods of time has had the effect of "shutting off" erosion locally during the time period of alluvial storage. Over the long term, alluvial storage will have the effect of lowering the "effective" bedrock erodibility. In order to include this effect, it is necessary to use a long-term "effective" measure of bedrock erosion (e.g., the total extent of headcutting along major side canyons, as is used here) rather than a short-term measure of erosion that may sample time periods during which there was significantly more, or less, alluvial storage. As long as the effective bedrock erodibility, K, is calibrated over sufficiently long time scales, the protective effect of episodic alluvial storage is implicitly included in the calibration.

Similarly, a sequence of trial and error was used to infer the value of $K'\tau$ most consistent with the observed longitudinal profile of the Colorado River in Grand Canyon. The values of K' were assumed to be proportional to K, hence the value of $K'\tau$ reduces to a critical value for $\tau = SA^{0.5}$. The modern Colorado River has a drainage area of 279,000 km^2 above Lees Ferry and a slope of ~10^{-4}. Therefore, the critical value of $SA^{0.5}$ must be less than the observed value of $SA^{0.5}$ = 0.53 km for the modern Colorado River. If the critical value of $SA^{0.5}$ is assumed to be zero, the Colorado River in western Grand Canyon develops a slope of ~3×10^{-5} by the end of the simulation, i.e., a value equal to roughly one-third of the actual value. The threshold value for $SA^{0.5}$ was systematically increased from zero during model calibration until the slope of the Colorado River in the model matched the observed slope in western Grand Canyon, simultaneously varying the absolute value of K as needed to maintain consistency with the observed extent of headcutting along Kanab and Havasu Creeks. The resulting best-fit threshold value of $SA^{0.5}$ was 0.25 km. More details on the sensitivity of the model to individual parameters are described in the Model Results section below.

Rates of retreat of the cliff-forming limestone units of Grand Canyon have been directly inferred by Cole and Mayer (1982) and Abbott and Lundstrom (2007) from latest Pleistocene time to the present. Cole and Mayer compared the spatial distribution of modern packrat middens to fossil middens in caves of the region. As cliffs retreat and middens near cave entrances are entrained by mass movement failures of the cliff wall, the population of middens in a cave becomes skewed toward younger ages. By quantifying this effect, Cole and Mayer (1982) were able to infer cliff retreat rates of 0.3–0.7 m/ka in the resistant limestone units of Grand Canyon, a range later confirmed by Abbott and Lundstrom (2007) using travertine deposits. Cosmogenic dating of cliff retreat rates in the Negev Desert also provide supporting evidence for the 0.3–0.7 m/ka range for arid-region cliffs comprised of resistant rock types (Matmon et al., 2005). In a large compilation study, Schmidt (1988) reported that most resistant rock types retreat at rates of ~0.5 m/ka in arid regions worldwide. In the model, I used C = 0.5 m/ka to quantify retreat rates (Fig. 6) in both the strong and weak rock units of the canyon. I used the same value of cliff retreat rates for both strong and weak units because, in a layered sequence, higher rates of cliff retreat lower down can have the effect of undercutting the strong units above them, thereby causing the strong units to retreat at rates similar to the weak units. Given that

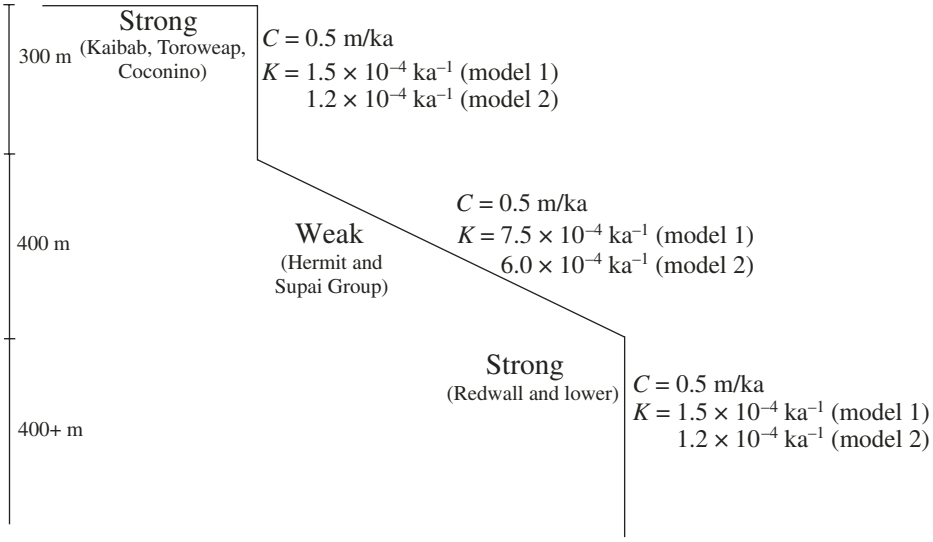

Figure 6. Schematic diagram illustrating the spatial variability of bedrock erodibilities and cliff retreat rates in the model. The coefficient of bedrock channel erodibility, K, is a function of the depth of incision into the rim surface, $h_{rs} - h$. If $h_{rs} - h < 300$ m, the value of K is a relatively high 1.5×10^{-4} ka^{-1} (model 1), corresponding to the strong units of the Kaibab through Coconino units. If $300 < h - h_{rs} < 700$ m, the value of K is a relatively high 7.5×10^{-4} ka^{-1}, corresponding to the weak units of the Hermit Shale and Supai Group. Finally, if $h - h_{rs} > 700$ m, $K = 1.5 \times 10^{-4}$ ka^{-1}, corresponding to the strong units of the Redwall Limestone and lower units. In model 2 (i.e., no erosion assumed prior to 6 Ma, the values of K are 1.2×10^{-4} ka^{-1} and 6.0×10^{-4} ka^{-1} for the strong and weak units of the Grand Canyon, respectively.

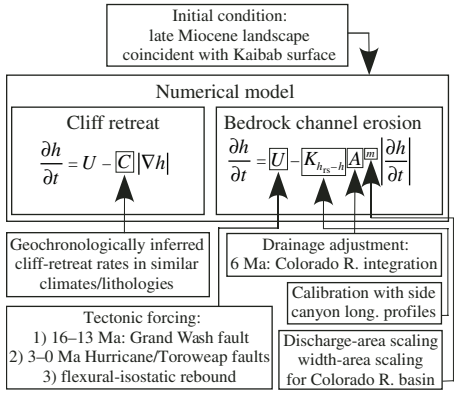

Figure 7. Schematic diagram illustrating the workflow of the model and its calibration. The coefficient K is written with a subscript $h_{rs} - h$ in order to emphasize that it is a function of $h_{rs} - h$, the depth of incision into the rim surface.

the measured late-Quaternary rates of cliff retreat in the resistant units of Grand Canyon is 0.5 m/ka, both the strong and weak units should be assigned the 0.5 m/ka value. It should be noted that rates of cliff retreat in nature depend on the height of the cliff and the dip of the underlying geologic unit (Schmidt, 1988). As such, using a constant rate of cliff retreat should be regarded as only a first-order approximation to a very complex geomorphic process. The components and calibration steps for the model are summarized in Figure 7.

MODEL RESULTS

Summary

Color maps of model topography (Fig. 8) illustrate the model-predicted history of river incision according to model 1 (i.e., 6–0 Ma incision following introduction of the Colorado River). Incision beginning downstream at the topographic step associated with offset along the Grand Wash–Wheeler Fault system initiates a large (700 m) knickpoint that propagates upstream at a rate of ~100 km/Ma (Fig. 10A) in this model. By 4 Ma the knickpoint propagates upstream past Muav Gorge. As the knickpoint propagates upstream, it initiates the retreat of cliffs adjacent to the river. The width of the canyon, therefore, is a function of the rate of cliff retreat of the strongest (i.e., rate limiting) lithologic units and the elapsed time since the knickpoint has passed a given point along the river. As the knickpoint propagates upstream, the channel profile develops into two distinct zones. The upper portion of the profile that includes the knickpoint remains steep while the lower portion develops into a graded profile controlled by the critical shear stress for erosion in the stream-power model. Differential erosion above and below the Redwall Limestone creates a topographic bench in the model prior to Plio-Quaternary faulting and flexural-isostatic uplift. This topographic bench correlates with the elevation of the Esplanade Platform. The pattern of knickpoint retreat in the model is broadly consistent with Gardner's (1983) observations of knickpoint retreat in an experimental channel comprised of homogeneous cohesive sediments. In his experiments, a steep knickpoint formed following base-level drop that retreated laterally while maintaining its shape in the uppermost portion. As the knickpoint migrated upstream it became shorter as a graded channel developed at its base. The slope of this graded channel correlates with the threshold shear stress required to erode the bed. At the end of the simulation, the elevation of the Colorado River at the upstream boundary is ~200 m higher than the actual elevation (Fig. 10A). Therefore, the model underestimates the amount of erosion that has actually taken place in eastern Grand and Marble Canyons by 100–200 m.

Figure 9 illustrates the corresponding results for model 2 (incision of a proto–Grand Canyon driven by a paleodrainage of 13,000 km^2). Offset along the Grand Wash Fault between 16 and 13 Ma produces a large knickpoint east of the Grand Wash–Wheeler Fault system in this model that propagates at rates of ~15 km/Ma from 16 to 6 Ma (Fig. 10B). By 6 Ma, the upper portion of this knickpoint has reached the eastern edge of the Shivwitz Plateau. Following integration of the Colorado River at 6 Ma, rates of knickpoint propagation increase by approximately a factor of 4 to 60 km/Ma. As in model 1, differential erosion above and below the Redwall Limestone creates a topographic bench that correlates with the Esplanade Platform. The extent of cliff retreat in western Grand Canyon is higher in model 2 compared to model 1 because more time has elapsed for cliffs to retreat. The post–6 Ma history of model 2 is broadly similar to model 1 (more details below) except that the rate of knickpoint retreat is slower in model 2 (60 km/Ma) compared to model 1 (100 km/Ma). Both models predict broadly similar responses to Plio-Quaternary fault offset and flexural-isostatic uplift (more details below). This similarity is significant because it illustrates that the lake-spillover and headward erosion (to a possible capture point less than 150 km upstream from the Grand Wash Fault) scenarios are both geomorphically plausible. There are differences between the two models, however, and those differences may be useful in distinguishing the two models based on comparison with measured data.

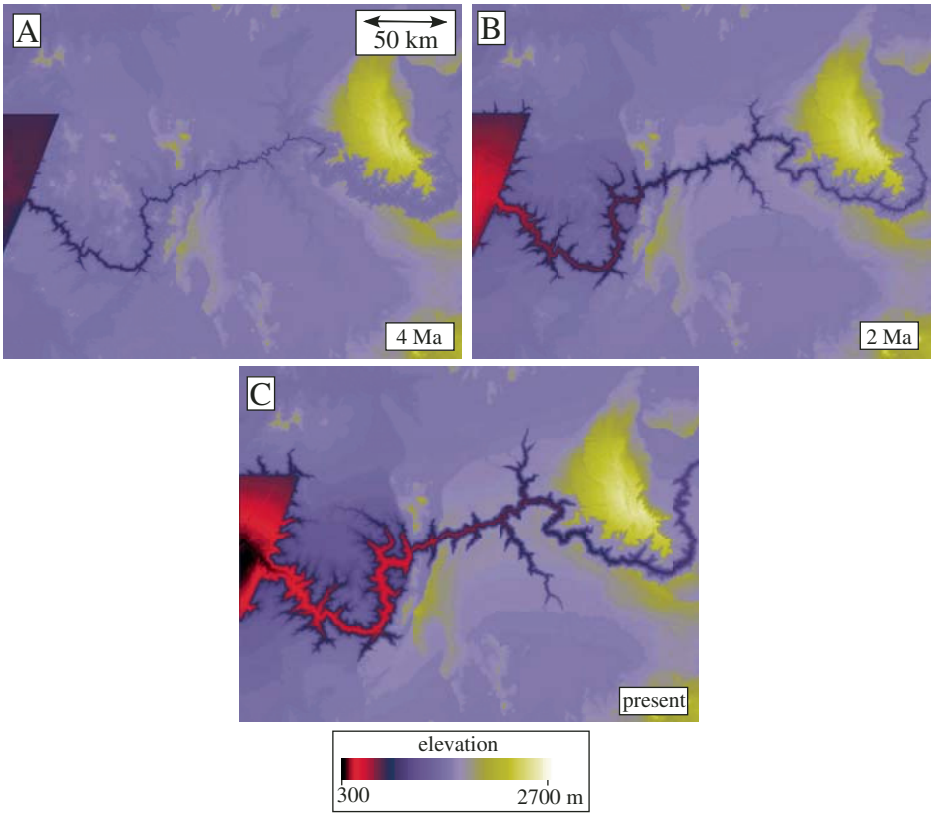

Figure 8. Color maps illustrating the topography predicted by model 1 for t = (A) 4 Ma, (B) 2 Ma, and (C) present. From 6 to 4 Ma, a large (700 m) knickpoint migrates headward at a rate of ~100 km/Ma to form a deep gorge in western Grand Canyon down to the level of the Redwall Limestone. By 4 Ma, the knickpoint has grown headward to a position east of Muav Gorge. From 4 to 2 Ma the knickpoint moves through eastern Grand and Marble Canyons. At the end of the model the canyon is wider in western Grand Canyon than in eastern Grand Canyon, reflecting the longer elapsed time since knickpoint retreat and the effect of fault-controlled subsidence of western Grand Canyon.

The planform geometry of Grand Canyon predicted by both models reproduces the extent of headward migration along the tributaries to Grand Canyon and the relative widths of western and eastern Grand Canyon quite well. Model 2, with its wider canyon overall, is more consistent with the observed topography compared to model 1, however. The relatively narrow width of the canyon in model 1 should not be interpreted as a rejection of the young canyon and lake-spillover hypothesis, however, because the width of the canyon depends sensitively on the rate of cliff retreat, which is not well constrained for pre-late Pleistocene climatic conditions. If cliff retreat rates in the Pliocene and early Quaternary were significantly greater than the rates inferred by Cole and Mayer (1982) for the late Pleistocene to the present, then the width of the canyon predicted by the model would be greater in both models. The greater width of western Grand Canyon compared to eastern Grand Canyon in both models is a consequence of the earlier age of incision in western Grand Canyon (hence the cliff walls in western Grand Canyon have had more time to retreat) as well as the subsidence that has dampened incision in this part of the canyon. Subsidence in western Grand Canyon means that bedrock channels in that portion of the canyon have not had to compete with rock uplift to the same extent as those in eastern Grand Canyon, hence they have grown headward at higher rates.

Determining the sensitivity of the model behavior to each input parameter provides a better understanding of the controls on Grand Canyon topography and the robustness of the model results. Figure 11 illustrates the sensitivity of model 2 to variations in each of the key model parameters (the sensitivity of model 1 is qualitatively similar to that of model 2). A 5% increase in the value of the drainage area exponent m (from 0.5 to 0.525) results in faster drainage network expansion, if all other parameters are kept fixed (Fig. 11A). A similar model result is obtained if the absolute value of the erodibility coefficient K is scaled up by 25%. In both cases, the resulting model topography is unrealistic—the canyons of Kanab and Havasu Creeks, for example, have eroded headward to distances tens of kilometers beyond the observed extent of deep headward incision in these canyons. The model sensitivity to variations in K is particularly important because the absolute value of this parameter is not independently constrained except by consistency with the modern topography. As such, it is important for the robustness of the model reconstruction that only a narrow range of K values are consistent with the modern extent of headcutting along the major side tributaries. Figure 11B illustrates the results of the model when no Plio-Quaternary normal faulting is included. Comparison of Figure 11B to Figure 10F illustrates that normal faulting has had the effect of widening western Grand Canyon relative to eastern Grand Canyon because bedrock channels in that portion of the canyon have not had to compete with rock uplift (due to Plio-Quaternary faulting) to the same extent as those in eastern Grand Canyon.

Constraints on Models for Colorado River Integration

The numerical models of this paper do not model the integration of the Colorado River explicitly. As such, they cannot constrain the mechanism of integration in detail. They can, however, address the geomorphic feasibility of different models for river integration and they can be used to evaluate proposed locations where integration may have occurred. The results of model 1 illustrate that lake spillover at 6 Ma can produce sufficient headcutting along the Colorado River to propagate the knickpoint to its modern location in the vicinity of Lees Ferry. The results of model 2 indicate that during Miocene time an incised drainage could have existed in western Grand Canyon large enough to have eroded headward to a position east of the Shivwitz Plateau by 6 Ma. The ability of this hypothesized paleodrainage in western Grand Canyon to grow headward is proportional to the square root of the drainage area in this model. As such, a drainage basin with an area only one-quarter as large as the one Young (2008) proposed would grow headward by a distance only half as great in the same time period (i.e., 75 km instead of 150 km in 10 Ma). As such, it is possible to conclude that a paleodrainage with an area much less than the one Young (2008) proposed could not have grown headward to a point east of the Shivwitz Plateau.

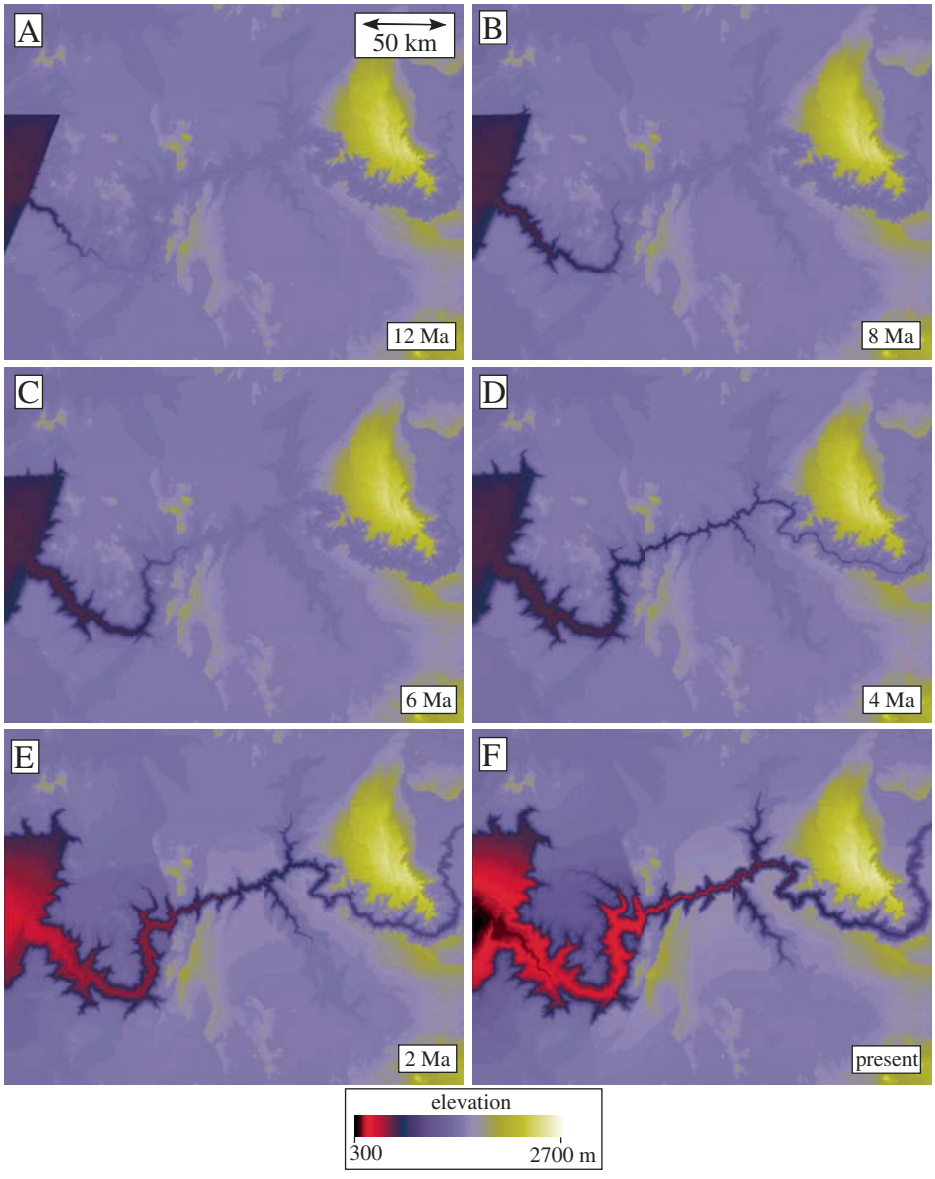

Figure 9. Color maps illustrating the topography predicted by model 2 for *t* = (A) 12 Ma, (B) 8 Ma, (C) 6 Ma, (D) 4 Ma, (E) 2 Ma, and (F) present. From 16 to 6 Ma, a large (700 m) knickpoint migrates headward at a rate of 15 km/Ma to form a deep gorge in western Grand Canyon. By 6 Ma, the knickpoint has grown headward to a position east of the Shivwitz Plateau. Following integration, the rate of knickpoint migration increases by a factor of 4, resulting in rapid incision of eastern Grand and Marble Canyons down to the level of the Redwall Limestone from 6 to 4 Ma. The canyon is several times wider in western Grand Canyon than in eastern Grand Canyon, as in model 1.

Similarly, the model rules out a drainage capture close to the Kaibab Monocline, as proposed by McKee et al. (1967), because such an event would have required headward migration of ~350 km instead of 150 km. Headward retreat of this extent would have required a drainage basin of ~50,000 km^2, i.e., much larger than any reasonable paleodrainage configuration. These results show that it is geomorphically possible for a paleodrainage of the size proposed by Young (2008) to capture an ancestral Colorado River east of the Shivwitz Plateau and west of Muav Gorge. As noted in the Introduction, however, most experts on the geology of this region agree that the limited volume of clastic debris deposited in the Grand Wash Trough and adjacent basins between 16.5 and 6 Ma rules out this hypothesis (e.g., Pederson et al., 2008).

The Role of Flexural-Isostatic Rebound on Grand Canyon Evolution

In both models, the excavation of rock from the Grand Canyon triggers isostatic rebound. Erosion occurs by both channel incision and cliff retreat in the model, but cliff retreat is responsible for the majority of rock removed. Because the rates of cliff retreat are similar in the two models, the spatial distribution and timing of isostatic rebound in the 6–0 Ma interval are also similar. As such, here I present results for isostatic rebound predicted by model 2 only. The rate of rock removal from Grand Canyon increases slowly through time in model 2 until 6 Ma (Fig. 9C); the rate then increases abruptly following the integration of the Colorado River. Figures 9C and 9D plot the fraction of the total volume of rock removed from the canyon system as a function of time in the two models. It may seem counterintuitive that the erosion rate should increase through time in these models—after all, the slopes of the bedrock channel system are *decreasing* through time as knickpoints propagate headward. However, most of the rock removed from the Grand Canyon is eroded by cliff retreat rather than by bedrock channel erosion. As the channels of the Grand Canyon system deepen and grow headward, the total area subject to cliff retreat increases. Since long-term rates of cliff retreat are two to three times greater than long-term rates of channel downcutting (i.e., 0.5 m/ka compared to 0.1–0.25 m/ka), the rate of total rock removal in Grand Canyon is controlled primarily by the cliff retreat process. The rate of total rock removal by cliff retreat will be approximately proportional to the total cliff area exposed along the canyon walls, which increases through time in both models 1 and 2.

Results of the flexural-isostatic component of model 2 indicate that incision in western Grand Canyon has triggered up to 350 m of rock uplift (Fig. 12), most of which would have occurred in Plio-Quaternary time due to the increase in the rate of rock removal through time (Fig. 9C). In model 1, the total isostatic rebound predicted by the model is ~20% lower than for model 2 (300 m of peak uplift compared to 350 m), but the spatial distribution of uplift is indistinguishable in the two models. Flexural-isostatic rebound occurs as a broad zone of uplift distributed over a zone of ~100 km centered on the Colorado River. Erosional unloading occurs over a relatively narrow zone compared to the flexural wavelength of the lithosphere. Because of the flexural rigidity of the lithosphere, however, isostatic rebound is spatially distributed over a broad

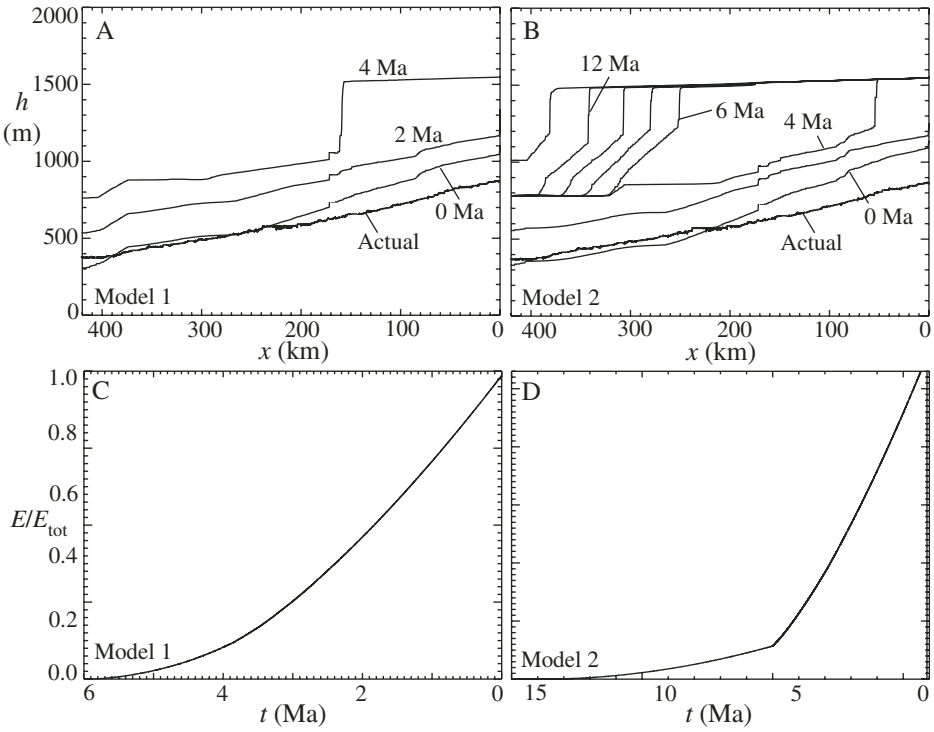

Figure 10. (A–B) Plots of the longitudinal profiles of the Colorado River (i.e., channel-bed elevation, *h*, as a function of along-channel distance downstream from Marble Canyon, *x*) predicted by models 1 and 2, respectively, in intervals of 2 Ma. Also shown is the actual profile extracted from 30 m/pixel U.S. Geological Survey digital elevation models (DEMs). (C–D) Plots of the rate of rock removal, E/E_{tot}, predicted by models 1 and 2 as a function of time, illustrating that most of the rock removed from the Grand Canyon in both models has occurred in Plio-Quaternary time. Although the overall gradient of the canyon system is decreasing through time, rock removal increases through time as downcutting and backwearing of the canyon system activates more area undergoing cliff retreat.

zone whose width is characterized by a width equal to approximately half of a flexural wavelength. The timing and magnitude of flexural isostatic rebound (i.e., up to 350 m of uplift over Plio-Quaternary time) are consistent with the timing and magnitude of uplift necessary to reproduce the observed rates of Quaternary incision in western Grand Canyon (i.e., 70 m/Ma). More details on Quaternary incision rates are discussed below. Model results also suggest that flexural-isostatic rebound has had a significant effect on the topography of the rim surface surrounding Grand Canyon. In the model topography, a broad topographic swell is predicted adjacent to the canyon rim in western and central Grand Canyon (Fig. 12B). It is difficult to be certain that the topographic swell observed in the actual topography (Fig. 12A) is due to flexural-isostatic uplift, but the swell observed in the DEM is consistent with the model prediction.

The results of both models suggest that Grand Canyon has evolved via a two-phased erosional response to the integration of the Colorado River. The onset of incision triggered the formation of a large knickpoint that propagated upstream through time. After the knickpoint propagates past a given point, a phase of cliff retreat begins that continues to the present. Cliff retreat leads to isostatic rebound, which triggers renewed incision of the Colorado River. This type of cyclic response is broadly analogous to Schumm's (1977) "complex response" of alluvial river channels to base-level drop. In Schumm's model, base-level lowering triggers knickpoint migration upstream. Channel widening by bank retreat following knickpoint passage lowers the stream power locally and promotes local aggradation. Local channel widening and aggradation eventually initiate renewed incision. In this way, alluvial channels undergo damped oscillations in sediment flux and the formation of multiple terrace levels in their response to a single episode of base-level drop. Cyclic models involving knickpoint retreat and flexural-isostatic response also have a long precedent in the geomorphic literature. In King and Pugh's model for the geomorphic evolution of southern Africa, for example, supercontinent breakup in the late Cretaceous triggered knickpoint propagation (King, 1956; Pugh, 1956). Erosional unloading associated with knickpoint propagation then triggered isostatic rebound and renewed knickpoint propagation. In this way, King and Pugh proposed that one regional tectonic event (e.g., supercontinent breakup) was responsible for the formation of multiple topographic levels in the landscape of southern Africa.

Plio-Quaternary Incision: Comparison between Model-Predicted and Geochronologically Measured Rates

Geochronologically derived Plio-Quaternary incision rates provide important constraints on the late Cenozoic geomorphic history of Grand Canyon. Depending on the offset datum (e.g., basalt flow, travertine deposit, fill terrace, etc.), these data represent incision rates over time scales from a few hundred thousand years to a few million years. Given the abundance of available data on Plio-Quaternary incision rates, it is useful to compare the model predictions for incision rates with observed patterns over the same time intervals, both as a model validation exercise and as a framework for better interpreting measured rates in terms of their underlying controls.

In the model, Plio-Quaternary incision rates reflect the final retreat of knickpoints through eastern Grand and Marble Canyons, flexural-isostatic rebound, and the effects of Plio-Quaternary normal faulting. At a given point along the river, incision rates are essentially zero until the knickpoint arrives, increases to a large value as the knickpoint passes, and then decreases to a "background" rate controlled by the rate of flexural-isostatic rebound plus the rate of fault-controlled rock uplift with respect to base level. Available geochronology data measure the average rate of incision over a given time interval, hence they may combine one or more of these incision phases.

Model-predicted incision rates yield patterns broadly similar to measured rates (Figs. 13A and 13B for models 1 and 2, respectively). For the measured data, I used all of the data compiled by Karlstrom et al. (2008) within Grand Canyon (shown as squares). Age uncertainties and/or uncertainties in the depth to bedrock introduce a two-sigma uncertainty value of ~20% in these data. The model-derived data for the time intervals 4–0 Ma and 2–0 Ma were obtained by differencing the elevation of the Colorado River between 4 and 0 Ma and 2 and 0 Ma, respectively, incorporating rock uplift relative to

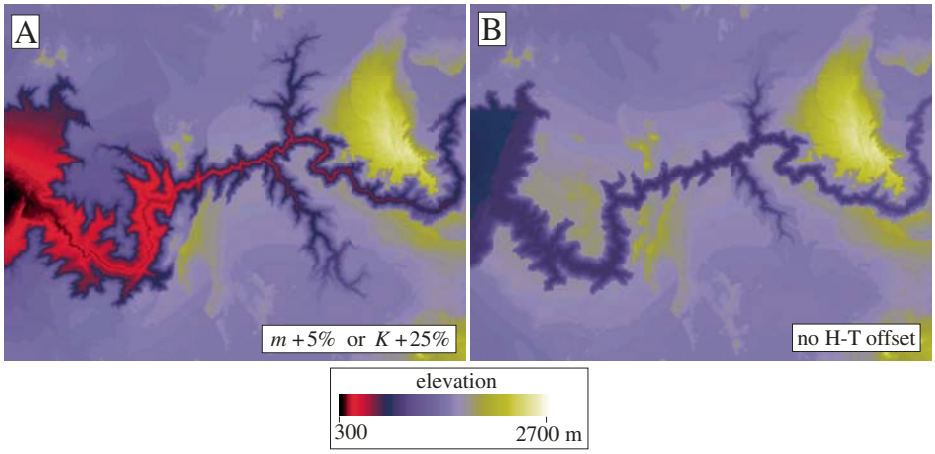

Figure 11. Color maps of the model predictions for modern topography according to variations of model 2, illustrating the sensitivity of the model results to individual parameters. (A) A 5% increase in the value of the drainage area exponent *m* or a 25% increase in the values of *K* results in unrealistic extensive knickpoint retreat along the major side canyons of Kanab and Havasu Creeks. (B) Eliminating the offset along the Hurricane and Toroweap Fault system results in a western Grand Canyon that is unrealistically narrower compared to the actual canyon.

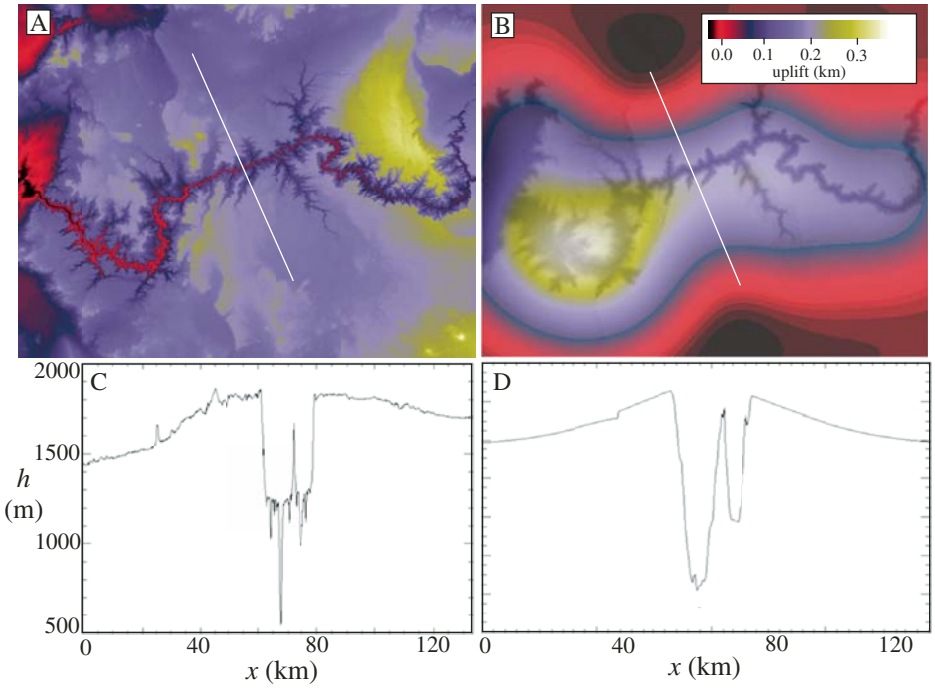

Figure 12. (A) Color map of the topography of the Grand Canyon region. (C) Cross-sectional topographic profile (from N to S) through the canyon at the location of Muav Gorge, illustrating the broad topographic swell that characterizes the plateau topography of western and central Grand Canyon. White line indicates the location of the profile. (B) Color map of total flexural-isostatic rebound predicted by model 2. (D) Cross-sectional topographic profile extracted from the model predicts a broad topographic swell similar to that observed in the actual topography at this location.

base level, and dividing the result by the duration of the time interval. Model 1 does a better job of predicting the relatively high rates of Plio-Quaternary incision in eastern Grand Canyon compared to model 2. In model 2, the knickpoint has already propagated past eastern Grand Canyon into Marble Canyon by 4 Ma (Fig. 10B). As such, knickpoint retreat influences incision in the post–4 Ma time period in Marble Canyon only in model 2 (Fig. 13B). The failure of model 2 to match measured incision rates in eastern Grand Canyon should not be used to rule out the proto–Grand Canyon hypothesis, however, because model-predicted incision rates are sensitive to the precise location of the knickpoint through time, which, in turn, is sensitive to model parameters (i.e., *K* and *m*) that are not precisely known. These results do suggest, however, that the rates of Plio-Quaternary incision measured in eastern Grand Canyon over the 4–0 Ma time interval likely include a knickpoint-passage component. The model suggests that flexural-isostatic rebound and fault incision alone could not have produced incision rates as high as 250 m/ka.

Modeled rates of Quaternary incision (2–0 Ma) in eastern Grand Canyon (maximum 150 m/Ma) are approximately twice as large as those in western Grand Canyon (maximum 70 m/Ma) in both models. This largely reflects the relative subsidence of western Grand Canyon, as proposed by Pederson et al. (2002). Incision rates in Grand Canyon are strongly controlled by uplift rates relative to base level (shown schematically in Fig. 13C). The uplift relative to base level is a combination of rock uplift due to fault offset and the flexural-isostatic response to erosional unloading. In western Grand Canyon downstream from the Hurricane Fault, the uplift relative to base level consists of the flexural-isostatic response (FIR) to erosion only (i.e., there is no Plio-Quaternary uplift along the Grand Wash Fault or any other fault between the Grand Wash Trough and the Hurricane Fault, hence no fault offset between the Grand Wash Trough and western Grand Canyon), which varies spatially in the model but has a maximum value of 70 m/Ma in western Grand Canyon. Between the Hurricane and Toroweap Faults, the uplift relative to base level consists of flexural-isostatic rebound plus the offset along the Hurricane Fault (i.e., ~100 m/Ma). East of the Toroweap Fault, the uplift relative to base level is equal to the flexural-isostatic response plus the combined offset along both faults. In far eastern Grand and Marble Canyons, remnant knickpoint propagation adds an additional component of incision based on the location of the knickpoint at the beginning of the time interval under consideration.

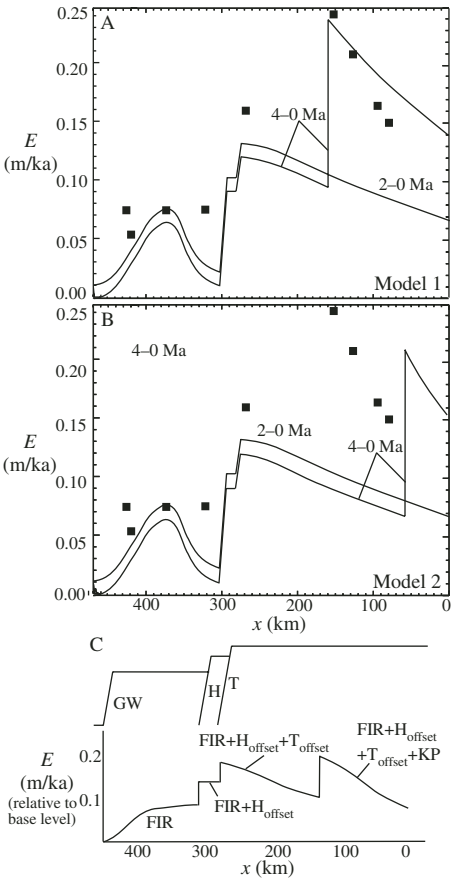

Figure 13. (A–B) Plots of Colorado River incision rate, *E* (m/ka), as a function of along-channel distance from Lees Ferry predicted by models 1 and 2, respectively. Two time intervals are included: 4–0 Ma and 2–0 Ma. These data show broadly similar patterns to those of incision rates determined geochronologically (data from Karlstrom et al. [2008] shown in squares), but model 1 is more consistent with the measured data in eastern Grand Canyon. (C) Schematic diagram of incisional response to rock uplift relative to base level, illustrating the effects of relative fault offset, flexural-isostatic rebound (FIR), and remnant knickpoint retreat (KP).

CONCLUSIONS

The late Cenozoic geomorphic evolution of Grand Canyon is controlled by mid-late Miocene and Plio-Quaternary phases of normal fault offset, bedrock channel erosion, cliff retreat, and flexural-isostatic response to erosional unloading. A model that combines these elements suggests that following Colorado River integration, incision took place as an eastward-propagating knickpoint with a velocity of ~100 km/Ma, resulting in rapid incision of western Grand Canyon down to the level of the Redwall Limestone from 6 to 4 Ma and eastern Grand and Marble Canyons from 4 to 2 Ma. Widening of Grand Canyon triggered flexural-isostatic rebound of up to 350 m, primarily in the Plio-Quaternary period. Plio-Quaternary normal faulting, however, acted in the opposite direction in western Grand Canyon, causing dampened incision in western Grand Canyon relative to eastern Grand Canyon, as proposed by Pederson et al. (2002).

An alternative end-member model scenario that includes a 13,000 km^2 paleodrainage in western Grand Canyon suggests that relief production along the Grand Wash Fault could have initiated the formation of a large (700-m-tall) knickpoint that migrated headward at a rate of 15 km/Ma to form a deep gorge in western Grand Canyon prior to Colorado River integration. This result is consistent with speleothem records of water-table lowering in western Grand Canyon (Hill et al., 2001; Polyak et al., 2008) and the Miocene paleogeography of the region as interpreted by Young (2008). Model results suggest that this proto–Grand Canyon initiated by offset along the Grand Wash–Wheeler Fault system could have grown headward to a position east of the Shivwitz Plateau by 6 Ma. Headward growth of this proto–Grand Canyon, therefore, could have been sufficiently rapid to capture the ancestral upper Colorado River, if it drained through the Kanab Plateau region west of the Kaibab Monocline and east of the Shivwitz Plateau, but it was not sufficient to capture the Colorado River, if it flowed southeast in the direction of the modern Little Colorado River as proposed by McKee et al. (1967). The limited volume of Miocene clastic debris in the Grand Wash Trough, however, still presents a problem for this hypothesis. If this hypothesis is correct, the proto–Grand Canyon must have been quite narrow, sediment derived from the proto–Grand Canyon must have been reworked to the ocean by a combination of eolian and fluvial processes, and/or significant sediment storage must have occurred within the canyon upstream from the Grand Wash Trough in late Miocene time.

ACKNOWLEDGMENTS

This work was partially supported by National Science Foundation grant EAR-0309518. I wish to thank Clem Chase, Phil Pearthree, and Cassie Fenton for helpful conversations on the geology of Grand Canyon and helpful reviews of the paper. Joel Pederson, Lawrence Plug, John Gosse, Bill Phillips, and Karl Karlstrom also provided critical reviews during the formal review process that greatly improved the paper.

REFERENCES CITED

Abbott, L.D., and Lundstrom, C., 2007, The use of travertine to measure rates of river incision and scarp retreat in the eastern Grand Canyon, Arizona: Geological Society of America Abstracts with Programs, v. 39, p. 484.

Aronsson, G., and Linde, K., 1982, Grand canyon—A quantitative approach to the erosion and weathering of stratified bedrock: Earth Surface Processes and Landforms, v. 7, p. 589–599, doi: 10.1002/esp.3290070607.

Baker, V.R., 2006, Paleoflood hydrology in a global context: Catena, v. 66, p. 161–168, doi: 10.1016/j.catena.2005.11.016.

Billingsley, G.H., and Wellmeyer, J.L., 2003, Geologic map of the Mount Trumbull 30° × 60° quadrangle, Mojave and Coconino Counties, northwestern Arizona: U.S. Geological Survey Geologic Investigations Series I-2766, map scale 1:100,000, 36 p.

Blackwelder, E., 1934, Origin of the Colorado River: Geological Society of America Bulletin, v. 45, p. 551–565.

Cole, K.L., and Mayer, L., 1982, Use of packrat middens to determine rates of cliff retreat in the eastern Grand Canyon, Arizona: Geology, v. 10, p. 597–599, doi: 10.1130/0091-7613(1982)10<597:UOPMTD>2.0.CO;2.

Cook, K.L., Whipple, K.X., Heimsath, A.M., and Hanks, T.C., 2009, Rapid incision of the Colorado River in Glen Canyon—Insights from channel profiles, local incision rates, and modeling of lithologic controls: Earth Surface Processes and Landforms, v. 34, p. 994–1010.

Crossey, L.J., Karlstrom, K.E., Springer, A., Newell, D., Hilton, D.R., and Fischer, T., 2009, Degassing of mantle-derived CO_2 and He from springs in the southern Colorado Plateau region—Neotectonic connections and implications for groundwater systems: Geological Society of America Bulletin (in press), doi: 10.1130/B26394.1.

Dallegge, T.A., Ort, M.H., McIntosh, W.E., and Perkins, M.E., 2001, Age and depositional basin morphology of the Bidahochi Formation and implications for the ancestral upper Colorado River, *in* Young, R.A., and Spamer, E.E., eds., The Colorado River: Origin and Evolution: Grand Canyon, Arizona, Grand Canyon Association Monograph 12, p. 47–51.

Davis, S.W., Davis, M.E., Lucchitta, I., Hanks, T.C., Finkel, R.C., and Caffee, M., 2001, Erosional history of the Colorado River through Glen and Grand Canyons, *in* Young, R.A., and Spamer, E.E., eds., The Colorado River: Origin and Evolution: Grand Canyon, Arizona, Grand Canyon Association Monograph 12, p. 135–140.

Faulds, J.E., Geissman, J.W., and Mawer, C.K., 1990, Structural development of a major extensional accommodation zone in the Basin and Range Province, northwestern Arizona and southern Nevada: Geological Society of America Memoir 176, p. 37–76.

Faulds, J.E., Price, L.M., and Wallace, M.A., 2001, Pre-Colorado River paleogeography and extension along the Colorado Plateau-Basin and Range boundary, northwest Arizona, *in* Young, R.A., and Spamer, E.E., eds., The Colorado River: Origin and Evolution: Grand Canyon, Arizona, Grand Canyon Association Monograph 12, p. 93–100.

Fenton, C.R., Webb, R.H., Pearthree, P.A., Cerling, T.E., and Poreda, R.J., 2001, Displacement rates on the Toroweap and Hurricane faults: Implications for Quaternary downcutting in the Grand Canyon, Arizona: Geology, v. 29, p. 1035–1038, doi: 10.1130/0091-7613(2001)029<1035:DROTTA>2.0.CO;2.

Finnegan, N.J., Roe, G., Montgomery, D.R., and Hallet, B., 2005, Controls on the channel width of rivers: Implications for modeling fluvial incision of bedrock: Geology, v. 33, p. 229–232, doi: 10.1130/G21171.1.

Flowers, R.M., Wernicke, B.P., and Farley, K.A., 2008, Unroofing, incision, and uplift history of the southwestern Colorado Plateau from apatite (U-Th)/He thermochronometry: Geological Society of America Bulletin, v. 120, p. 571–587, doi: 10.1130/B26231.1.

Freeman, G.T., 1991, Calculating catchment area with divergent flow based on a rectangular grid: Computers and Geosciences, v. 17, p. 413–422, doi: 10.1016/0098-3004(91)90048-I.

Gardner, T.W., 1983, Experimental study of knickpoint and longitudinal profile evolution in cohesive, homogeneous material: Geological Society of America Bulletin, v. 94, p. 664–672, doi: 10.1130/0016-7606(1983)94<664:ESOKAL>2.0.CO;2.

Hanks, T.C., and Blair, J.L., 2002, Comment on Pederson et al., 2002: Geology, v. 31, p. e16–e17.

Hanks, T.C., Lucchitta, I., Davis, S.W., Davis, M.E., Finkel, R.C., Lefton, S.A., and Garvin, C.D., 2001, The Colorado River and the age of Glen Canyon, *in* Young, R.A., and Spamer, E.E., eds., The Colorado River: Origin and Evolution: Grand Canyon, Arizona, Grand Canyon Association Monograph 12, p. 129–134.

Hereford, R., Thompson, K.S., and Burke, K.J., 1998, Numerical ages of Holocene tributary debris fans inferred from dissolution pitting on carbonate boulders in the Grand Canyon of Arizona: Quaternary Research, v. 50, p. 139–147, doi: 10.1006/qres.1998.1987.

Hill, C.A., Polyak, V.J., McIntosh, W.C., and Provencio, P.P., 2001, Preliminary evidence from Grand Canyon caves and mines for the evolution of Grand Canyon and the Colorado River system, *in* Young, R.A., and Spamer, E.E., eds., The Colorado River: Origin and Evolution: Grand Canyon, Arizona, Grand Canyon Association Monograph 12, p. 141–146.

Hill, C.A., Eberz, N., and Buecher, R.H., 2008, A karst connection model for Grand Canyon, Arizona: Geomorphology, v. 95, p. 316–334, doi: 10.1016/j.geomorph.2007.06.009.

Howard, K.A., Lundstrom, S.C., Malmon, D.V., and Hook, S.J., 2008, Age, distribution, and formation of late Cenozoic paleovalleys of the lower Colorado River and their relation to river aggradation and degradation *in* Reheis et al., ed., Late Cenozoic Drainage History in the Southwestern Great Basin and Lower Colorado River Region: Geologic and Biotic Perspectives: Geological Society of America Special Paper 439, p. 391–410.

Jackson, G., 1990, Tectonic geomorphology of the Toroweap fault, western Grand Canyon: Implications for the transgression of faulting on the Colorado Plateau: Arizona Geological Survey Open-File Report 90-4, 67 p.

Karlstrom, K.E., and Kirby, E., 2004, Colorado River system of the southwestern U.S.: Longitudinal profiles, differential incision, and a hypothesis for Quaternary tectonism at both ends: Geological Society of America Abstracts with Programs, v. 36, p. 550.

Karlstrom, K.E., Crow, R.S., Peters, L., McIntosh, W., Raucci, J., Crossey, L.J., Umhoefer, P., and Dunbar, N., 2007, $^{40}Ar/^{39}Ar$ and field studies of Quaternary basalts in Grand Canyon and model for carving Grand Canyon: Quantifying the interaction of river incision and normal faulting across the western edge of the Colorado Plateau: Geological Society of America Bulletin, v. 119, p. 1283–1312.

Karlstrom, K.E., Crow, R.S., Crossey, L.J., Coblentz, D., and van Wijk, J.W., 2008, Model for tectonically driven incision of the younger than 6 Ma Grand Canyon: Geology, v. 36, p. 835–838.

King, L.C., 1956, Pediplanation and isostasy, an example from South Africa: The Geological Society of London, v. 111, p. 353–359.

Lange, A., 1959, Introductory notes on the changing geometry of cave structures: Cave Studies, v. 11, p. 69–90.

Lee, J.P., 2007, Cenozoic unroofing of the Grand Canyon region, Arizona [M.S. thesis]: Lawrence, University of Kansas, 119 p.

Longwell, C.R., 1946, How old is the Colorado River?: American Journal of Science, v. 244, no. 12, p. 817–835.

Lowry, A.R., and Smith, R.B., 1995, Strength and rheology of the western U.S: Cordillera: Journal of Geophysical Research, v. 100, p. 17,947–17,963, doi: 10.1029/95JB00747.

Lowry, A.R., Ribe, N.M., and Smith, R.B., 2000, Dynamic elevation of the Cordillera, western United States: Journal of Geophysical Research, v. 105, p. 23,371–23,390, doi: 10.1029/2000JB900182.

Luke, J.C., 1972, Mathematical models for landform evolution: Journal of Geophysical Research, v. 77, p. 2460–2464, doi: 10.1029/JB077i014p02460.

Matmon, A., Shaked, Y., Porat, N., Enzel, Y., Finkel, R., Lifton, N., Boaretto, E., and Agnon, A., 2005, Landscape development in an hyperarid sandstone environment along the margins of the Dead Sea fault: Implications from dated rock falls: Earth and Planetary Science Letters, v. 240, p. 803–817, doi: 10.1016/j.epsl.2005.06.059.

McKee, E.D., Wilson, R.F., Breed, W.J., and Breed, C.S., eds., 1967, Evolution of the Colorado River in Arizona: Museum of Northern Arizona Bulletin 44, 67 p.

Meek, N., and Douglass, J., 2001, Lake overflow: An alternative hypothesis for Grand Canyon incision and development of the Colorado River, *in* Young, R.A., and Spamer, E.E., eds., The Colorado River: Origin and Evolution: Grand Canyon, Arizona, Grand Canyon Association Monograph 12, p. 199–206.

Pearthree, P.A., Spencer, J.E., Faulds, J.E., and House, P.K., 2008, Comment on age and evolution of Grand Canyon revealed by U-Pb dating of water table-type speleothems: Science, v. 321, p. 1634e, doi: 10.1126/science.1158862.

Pederson, J.L., 2008, The mystery of the pre-Grand Canyon Colorado River—Results from the Muddy Creek Formation: GSA Today, v. 18, p. 4–10, doi: 10.1130/GSAT01803A.1.

Pederson, J., Karlstrom, K., Sharp, W., and McIntosh, W., 2002, Differential incision of the Grand Canyon related to Quaternary faulting—Constraints from U-series and Ar/Ar dating: Geology, v. 30, p. 739–742, doi: 10.1130/0091-7613(2002)030<0739:DIOTGC>2.0.CO;2.

Pederson, J.L., Schmidt, J.C., and Anders, M.D., 2003, Pleistocene and Holocene geomorphology of Marble and Grand Canyons, canyon cutting to adaptive management, *in* Easterbrook, D.J., ed., Quaternary Geology of the United States: Reno, Nevada, International Union for Quaternary Research, 2003 Field Guide Volume, Desert Research Institute, p. 407–438.

Pederson, J.L., Anders, M.D., Rittenour, T.M., Sharp, W.D., Gosse, J.C., and Karlstrom, K.E., 2006, Using fill terraces to understand incision rates and evolution of the Colorado River in eastern Grand Canyon, Arizona: Journal of Geophysical Research, v. 111, p. F02003, doi: 10.1029/2004JF000201.

Pederson, J., Young, R., Lucchitta, I., Beard, S.L., and Billingsley, G., 2008, Comment on age and evolution of Grand Canyon revealed by U-Pb dating of water table-type speleothems: Science, v. 321, p. 1634b, doi: 10.1126/science.1158019.

Pelletier, J.D., 2007, Numerical modeling of the Cenozoic fluvial evolution of the southern Sierra Nevada, California: Earth and Planetary Science Letters, v. 259, p. 85–96, doi: 10.1016/j.epsl.2007.04.030.

Pelletier, J.D., 2008, Quantitative Modeling of Earth Surface Processes: New York, Cambridge University Press, 295 p.

Pollack, H.N., 1969, A numerical model of the Grand Canyon, *in* Baars, D.L., ed., Geology and Natural History of the Grand Canyon Region: Guidebook for the Fifth Field Conference, Four Corners Geological Society, p. 61–62.

Polyak, V.J., Hill, C.A., and Asmerom, Y., 2008, Age and evolution of the Grand Canyon revealed by U-Pb dating of water table-type speleothems: Science, v. 319, p. 1377–1380, doi: 10.1126/science.1151248.

Press, W.H., Flannery, B.P., and Teukolsky, S.A., 1992, Numerical recipes in C (second edition): New York, Cambridge University Press, 400 p.

Pugh, J.C., 1956, Isostatic readjustment in the theory of pediplanation: The Geological Society of London, v. 111, p. 361–374.

Scarborough, R., 2001, Neogene development of the Little Colorado River Valley and eastern Grand Canyon: Field evidence for an overtopping hypothesis, *in* Young, R.A., and Spamer, E.E., eds., The Colorado River: Origin and Evolution: Grand Canyon, Arizona, Grand Canyon Association Monograph 12, p. 207–214.

Schmidt, K.H., 1988, Rates of scarp retreat: A means of dating Neotectonic activity, *in* Jacobshagen, V.H., ed., The Atlas System of Morocco: Studies on its Geodynamic Evolution, Lecture Notes in Earth Science, v. 15, p. 445–462.

Schumm, S.A., 1977, The Fluvial System: New York, John Wiley and Sons.

Sklar, L., and Dietrich, W.E., 2004, A mechanistic model for river incision into bedrock by saltating bedload: Water Resources Research, v. 40, doi: 10.1029/2003WR002496.

Spencer, J.E., and Pearthree, P.A., 2001, Headward erosion versus closed-basin spillover as alternative causes of Neogene capture of the ancestral Colorado River by the Gulf of California, *in* Young, R.A., and Spamer, E.E., eds., The Colorado River: Origin and Evolution: Grand Canyon, Arizona, Grand Canyon Association Monograph 12, p. 215–222.

Spencer, J.E., Peters, L., McIntosh, W.C., and Patchett, P.J., 1998, 6 Ma Ar/Ar date from the Hualapai Limestone and implications for the age of the Bouse formation and Colorado River: Geological Society of America Abstracts with Programs, v. 30, p. 37.

Tucker, G.E., and Bras, R.L., 1998, Hillslope processes, drainage density, and landscape morphology: Water Resources Research, v. 34, p. 2751–2764, doi: 10.1029/98WR01474.

Watts, A.B., 2001, Isostasy and flexure of the lithosphere: Cambridge, Cambridge University Press, 458 p.

Wenrich, K.J., Billingsley, G.H., and Huntoon, P.W., 1997, Breccia-pipe and geologic map of the northeastern part of the Hualapai Indian reservation and vicinity, Arizona: U.S. Geological Survey Miscellaneous Investigations Map I-2440, scale 1:48000, 19 p.

Whipple, K.X., 2004, Bedrock rivers and the geomorphology of active orogens: Annual Review of Earth and Planetary Sciences, v. 32, p. 151–185, doi: 10.1146/annurev.earth.32.101802.120356.

Whipple, K.X., and Tucker, G.E., 1999, Dynamics of the stream-power river incision model: Implications for height limits of mountain ranges, landscape response timescales, and research needs: Journal of Geophysical Research, v. 104, p. 17,661–17,674, doi: 10.1029/1999JB900120.

Whipple, K.X., Hancock, G.S., and Anderson, R.S., 2000, River incision into bedrock: Mechanics and relative efficacy of plucking, abrasion, and cavitation: Geological Society of America Bulletin, v. 112, p. 490–503, doi: 10.1130/0016-7606(2000)112<0490:RIIBMA>2.3.CO;2.

Whittaker, A.C., Cowie, P.A., Attal, M., Tucker, G.E., and Roberts, G.P., 2007, Bedrock channel adjustment to tectonic forcing: Implications for predicting river incision rates: Geology, v. 35, p. 103–106, doi: 10.1130/G23106A.1.

Wohl, E., and David, G.C.L., 2008, Consistency of scaling relations among bedrock and alluvial channels: Journal of Geophysical Research, v. 113, p. F04013, doi: 10.1029/2008JF000989.

Wolkowinsky, A.J., and Granger, D.E., 2004, Early Pleistocene incision of the San Juan River, Utah, dated with 26Al and 10Be: Geology, v. 32, p. 749–752, doi: 10.1130/G20541.1.

Young, R.A., 2008, Pre-Colorado River drainage in western Grand Canyon: Potential influence on Miocene stratigraphy in Grand Wash Trough, *in* Reheis et al., eds., Late Cenozoic Drainage History in the Southwestern Great Basin and Lower Colorado River Region: Geologic and Biotic Perspectives: Geological Society of America Special Paper 439, p. 319–333.

Manuscript Received 7 January 2008
Revised Manuscript Received 15 April 2009
Manuscript Accepted 23 April 2009

Printed in the USA